

Imperfect nesting in spin-density waves

Xiaozhou Huang* and Kazumi Maki

Department of Physics, University of Southern California, Los Angeles, California 90089-0484

(Received 29 August 1991)

We study theoretically the effects of imperfect nesting in spin-density waves (SDW's) in quasi-one-dimensional systems. We analyze the phase diagram, the specific heat, and the threshold electric field in the presence of imperfect nesting. The latter result appears to describe the temperature dependence of the threshold electric field observed in SDW's of quenched di-tetramethyl-tetraselena-fulvalene chlorate [(TMTSF)₂ClO₄] observed by Shimizu *et al.*

I. INTRODUCTION

For a long time it has been assumed that the charge-density wave (CDW) and spin-density wave (SDW) found in quasi-one-dimensional systems are essentially one dimensional, since the energy gap extracted from the electric conductivity of a typical CDW is much larger than the value expected from the mean-field theory.¹ This discrepancy was usually ascribed to the large fluctuation or the strong coupling in the one-dimensional systems. Further, the observed peak in the temperature derivative of the electric conductivity² at the CDW transition temperature gave the one-dimensional fluctuation, if it is interpreted in terms of the theory put forward by Horn and Guiddoti.³ However, one of us discovered⁴ recently that the theory by Horn and Guiddoti does not apply to CDW's of NbSe₃, since these compounds are usually in the clean limit. Then in light of our theory, the same data are interpreted as due to the three-dimensional fluctuation.⁴ In general, the effect of the fluctuation is not large and treated within the loop expansion. As to the large ratio of $2\Delta_a/T_c$ observed in CDW's where Δ_a is the apparent energy gap, it is realized that this is due to imperfect nesting. Making use of an early model proposed by Horowitz, Weger, and Gutfreund,⁵ and a parallel model used by Yamaji⁶ for SDW, we are able to interpret⁷ the large ratio of $2\Delta_a/T_c$ and the pressure dependence of T_c in NbSe₃ observed by Briggs *et al.*⁸ Indeed, we can describe the temperature dependence of $\Delta_a(T)$ determined from the electron-tunneling density of states in CDW's in NbSe₃ by Ekino and Akimitsu⁹ in terms of the three-dimensional model with imperfect nesting. Therefore, the mean-field theory appears to be adequate to describe CDW's, though the detailed comparison between theory and experiment is so far limited to NbSe₃.⁷

As to SDW, $2\Delta_a/T_c$ in SDW of di-tetramethyl-tetraselena-fulvalene hexafluoro-phosphate [(TMTSF)₂PF₆] is close to the BCS value¹⁰ which implies small imperfect nesting. Further, Yamaji⁶ has already described the pressure dependence of the SDW-transition temperature T_c (Ref. 11) observed in (TMTSF)₂PF₆ in terms of increase in imperfect nesting due to the pressure. More recently, the same model is shown to describe many features of the field-induced spin-density waves¹²⁻¹⁴ ob-

served in (TMTSF)₂ClO₄ and (TMTSF)₂PF₆ under high pressure ($P \sim 7 \sim 8$ k bar) in high magnetic fields ($5 < H < 30T$). Some of predictions¹⁵⁻¹⁸ made based on Yamaji's model (i.e., anisotropic Hubbard model) wait the experimental verification. We note in passing that the temperature dependence of the threshold electric field¹⁹ associated with nonohmic conduction observed in SDW's of both pristine and x-ray irradiated samples of (TMTSF)₂PF₆ is well described in terms of the model with small imperfect nesting.²⁰ Very recently, Shimizu *et al.*²¹ reported observation of the threshold electric field in SDW of quenched (TMTSF)₂ClO₄. Unlike SDW (Ref. 22) in (TMTSF)₂NO₃ and (TMTSF)₂PF₆, the threshold electric field in this SDW exhibits much stronger temperature dependence.

The object of this paper is to extend our analysis of the effects of imperfect nesting to thermodynamics and the threshold electric field for large imperfect nesting. We found that the model with large imperfect nesting indeed describes the strong temperature dependence of the threshold electric field as found in quenched (TMTSF)₂ClO₄.

II. THERMODYNAMICS

Although the thermodynamics of the present model has been already described by a few authors,^{6,16} we reanalyzed it here, since we have found simple analytical expressions for free energy, etc., which apply in the limit of large imperfect nesting ($\epsilon_0 > \Delta$ where ϵ_0 is the parameter characterizing the imperfect nesting and Δ is the SDW order parameter). Also, most of the present results apply as well for CDW. However, we limit ourselves to SDW for simplicity. The Hamiltonian we study is given by

$$H = \sum_{p,\alpha} \epsilon(p) c_{p\alpha}^\dagger c_{p\alpha} + U \sum_q n_{q\uparrow} n_{-q\downarrow}, \quad (1)$$

where

$$\begin{aligned} \epsilon(p) &= -2t_a \cos(ap_1) - 2t_b \cos(bp_2) \\ &\quad - 2t_c \cos(cp_3) - \mu \\ &\simeq v(|p_1| - p_F) - 2t_b \cos(bp_2) \\ &\quad - \epsilon_0 \cos(2bp_2) - 2t_c \cos(cp_3), \end{aligned} \quad (2)$$

with

$$\varepsilon_0 = -\frac{1}{2}t_b^2 \cos(ap_F) [t_a \sin^2(ap_F)]^{-1}. \quad (3)$$

Here $c_{p\alpha}^\dagger$ and $c_{p\alpha}$ are the electron creation and annihilation operators with momentum \mathbf{p} and spin α ($=\uparrow$ or \downarrow) and $n_{q\uparrow}$ and $n_{q\downarrow}$ are the corresponding density operators. We introduced an approximation^{6,15} for the quasiparticle energy, which is valid in the vicinity of the Fermi surface and when $t_a \gg t_b \gg t_c$. Then for not too large ε_0 , the ground state of the Hamiltonian is SDW with nesting vector $\mathbf{Q}=(2p_F, \pi/b, \pi/c)$ and the quasiparticle Green's function is given by

$$G^{-1} = i\omega_n - \eta - \xi\rho_3 - \Delta\rho_1\sigma_3, \quad (4)$$

where

$$\xi = v(|p_1| - p_F) - 2t_b \cos(bp_2) - 2t_c \cos(cp_3), \quad (5)$$

$$\eta = \varepsilon_0 \cos(2bp_2),$$

and ω_n is the Matsubara frequency and ρ_i 's are the Pauli matrices operating on the spinor space formed by the right-going and the left-going electrons. The gap equation is now written as

$$\begin{aligned} 2\bar{U}^{-1} &= \pi T \sum_n \left\langle [(\omega_n + i\eta)^2 + \Delta^2]^{-1/2} \right\rangle \\ &= \ln(2E_c/\Delta) - 2 \sum_{n=1}^{\infty} (-1)^{n+1} K_0(n\beta\Delta) I_0(n\beta\varepsilon_0) \end{aligned} \quad (6a)$$

$$\begin{aligned} &= \ln(2E_c/\varepsilon_0) - 2 \sum_{n=1}^{\infty} (-1)^{n+1} I_0(n\beta\Delta) K_0(n\beta\varepsilon_0), \end{aligned} \quad (6b)$$

where $\bar{U} = UN_0$, $N_0 = (\pi vbc)^{-1}$ is the electron density of states at the Fermi surface per spin, and $\langle \rangle$ means average over $\phi = bp_2$, E_c is the cutoff energy, and $I_0(z)$ and $K_0(z)$ are the modified Bessel functions. The symmetry between Δ and ε_0 as seen between Eqs. (6a) and (6b) follows from the relation

$$F = \begin{cases} -N_0 \left\{ \frac{1}{2}(\Delta^2 - \varepsilon_0^2) + 2\Delta^2 \sum_{n=1}^{\infty} (-1)^{n+1} K_2(n\beta\Delta) I_0(n\beta\varepsilon_0) \right\} & \text{for } \Delta > \varepsilon_0, \end{cases} \quad (9a)$$

$$F = \begin{cases} -N_0 \left\{ \frac{1}{3}(\pi T)^2 + 2\Delta^2 \sum_{n=1}^{\infty} (-1)^{n+1} I_2(n\beta\Delta) K_0(n\beta\varepsilon_0) \right\} & \text{for } \Delta < \varepsilon_0, \end{cases} \quad (9b)$$

$$S = \begin{cases} 4N_0\beta\Delta \sum_{n=1}^{\infty} (-1)^{n+1} [\Delta K_2(n\beta\Delta) I_0(n\beta\varepsilon_0) - \varepsilon_0 K_1(n\beta\Delta) I_1(n\beta\varepsilon_0)] & \text{for } \Delta > \varepsilon_0, \end{cases} \quad (10a)$$

$$S = \begin{cases} N_0 \left\{ \frac{2}{3}\pi^2 T + 4\beta\Delta \sum_{n=1}^{\infty} (-1)^{n+1} [\Delta I_2(n\beta\Delta) K_0(n\beta\varepsilon_0) - \varepsilon_0 I_1(n\beta\Delta) K_1(n\beta\varepsilon_0)] \right\} & \text{for } \Delta < \varepsilon_0, \end{cases} \quad (10b)$$

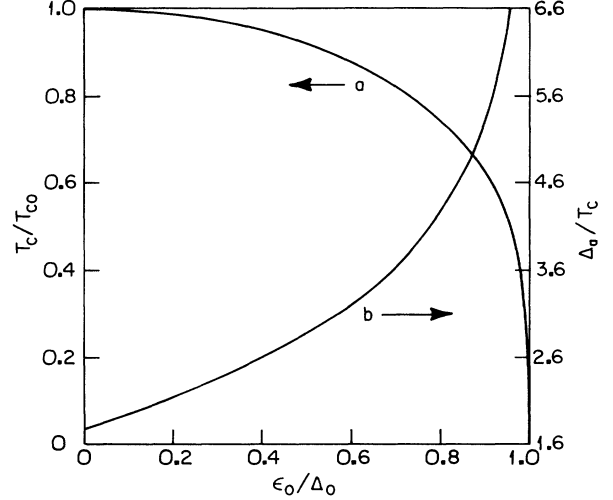


FIG. 1. (a) T_c/T_{c0} and (b) Δ_a/T_c are shown as functions of ε_0/Δ_0 , where T_c and Δ_a is the SDW transition temperature and the apparent energy gap when $\varepsilon_0 \neq 0$ and Δ_0 is the SDW order parameter at $T=0$ K.

$$\begin{aligned} &\int \int_0^{2\pi} \frac{d\phi dx}{(2\pi)^2} (a + ib \cos\phi + ic \cos x)^{-1} \\ &= \int_0^{2\pi} \frac{d\phi}{2\pi} [(a + ib \cos\phi)^2 + c^2]^{-1/2} \\ &= \int_0^{2\pi} \frac{dx}{2\pi} [(a + ic \cos x)^2 + b^2]^{-1/2}. \end{aligned} \quad (7)$$

Further, Eq. (6a) gives a convergent series for $\varepsilon_0 < \Delta$, while Eq. (6b) for $\varepsilon_0 > \Delta$. One of the consequences of this symmetry is that the SDW transition temperature T_c in the presence of ε_0 is given by

$$\Delta(T_c/T_{c0}) = \varepsilon_0, \quad (8)$$

where T_{c0} is the transition temperature for $\varepsilon_0=0$ and $\Delta(T/T_{c0})$ is the temperature-dependent order parameter when $\varepsilon_0=0$. T_c/T_{c0} and Δ_a/T_c are shown in Fig. 1 as function of ε_0/Δ_0 where Δ_0 is the order parameter at $T=0$ K and $\Delta_a = \Delta + \varepsilon_0$ (i.e., the peak in the electron density of states⁷).

Following the standard procedure²³ the thermodynamic functions are constructed from Eqs. (6a) and (6b).

$$C_s = \begin{cases} N_0 \left\{ -2\Delta \frac{d\Delta}{dT} + 4\beta\Delta \sum_{n=1}^{\infty} (-1)^{n+1} \{ \Delta K_2(n\beta\Delta) [I_0(n\beta\epsilon_0) - n\beta\epsilon_0 I_1(n\beta\epsilon_0)] \right. \\ \left. - \epsilon_0 K_1(n\beta\Delta) [I_1(n\beta\epsilon_0) - n\beta\epsilon_0 I_0(n\beta\epsilon_0)] \} \right\} & \text{for } \Delta > \epsilon_0, \\ N_0 \left\{ \frac{2}{3} \pi^2 T - 4\beta\epsilon_0 \Delta \frac{d\Delta}{dT} \sum_{n=1}^{\infty} (-1)^{n+1} n I_0(n\beta\epsilon_0) K_1(n\beta\epsilon_0) \right. \\ \left. + 4\beta\Delta \sum_{n=1}^{\infty} (-1)^{n+1} \{ \Delta I_2(n\beta\Delta) [K_0(n\beta\epsilon_0) + n\beta\epsilon_0 K_1(n\beta\epsilon_0)] \right. \\ \left. - \epsilon_0 I_1(n\beta\Delta) [K_1(n\beta\epsilon_0) + n\beta\epsilon_0 K_0(n\beta\epsilon_0)] \} \right\} & \text{for } \Delta < \epsilon_0. \end{cases} \quad (11a)$$

$$C_s = \begin{cases} N_0 \left\{ \frac{2}{3} \pi^2 T - 4\beta\epsilon_0 \Delta \frac{d\Delta}{dT} \sum_{n=1}^{\infty} (-1)^{n+1} n I_0(n\beta\epsilon_0) K_1(n\beta\epsilon_0) \right. \\ \left. + 4\beta\Delta \sum_{n=1}^{\infty} (-1)^{n+1} \{ \Delta I_2(n\beta\Delta) [K_0(n\beta\epsilon_0) + n\beta\epsilon_0 K_1(n\beta\epsilon_0)] \right. \\ \left. - \epsilon_0 I_1(n\beta\Delta) [K_1(n\beta\epsilon_0) + n\beta\epsilon_0 K_0(n\beta\epsilon_0)] \} \right\} & \text{for } \Delta < \epsilon_0. \end{cases} \quad (11b)$$

In particular, the jump in the specific heat at $T = T_c(\epsilon_0)$ is given by

$$\begin{aligned} \Delta C_s &= \frac{1}{2} N_0 \beta \left[\frac{d\Delta^2}{dT} \Big|_{T=T_c} \right]^2 \sum_{n=1}^{\infty} (-1)^{n+1} n^2 K_0(n\beta\epsilon_0) \\ &= \frac{1}{2} N_0 \beta \epsilon_0^2 \left[\sum_{n=1}^{\infty} (-1)^{n+1} n K_1(n\beta\epsilon_0) \right]^2 / \sum_{n=1}^{\infty} (-1)^{n+1} n^2 K_0(n\beta\epsilon_0). \end{aligned} \quad (12)$$

Making use of Eqs. (9a), (9b), (11a), and (11b), the free energy and the specific heat of SDW are calculated. For example, the phase boundary between SDW and the superconducting state is determined when $F = F_{sc}$ where F_{sc} is the free energy of the BCS state if we assume that the superconducting state in Bechgaard salts is an ordinary S -wave state.⁶ F_{sc} is obtained from Eq. (9a) by putting $\epsilon_0 = 0$ and changing T_{c0} to T_{sc} the superconducting transition temperature. We show in Fig. 2 the temperature dependence of F for a few ϵ_0 's and in Fig. 3 the phase boundary between SDW and the superconducting state when $T_{sc}/T_{c0} = 0.25$ and 0.15 . The phase boundary is quite similar to the one determined by Yamaji⁶ earlier, except perhaps a somewhat sharper slope near $T = T_{sc}$. The specific heat is evaluated for a few ϵ_0/Δ_0 and shown as function of T/T_c in Fig. 4. The jump in specific heat decreases with increasing ϵ_0 as already predicted by Montambaux.¹⁶ It appears that the specific heat takes the same value independent of ϵ_0/Δ_0 when $T/T_c \simeq 0.55$.

$$f_1 = \begin{cases} 1 - 2\beta\Delta \sum_{n=1}^{\infty} (-1)^{n+1} n K_1(n\beta\Delta) I_0(n\beta\epsilon_0) & \text{for } \Delta > \epsilon_0, \\ 2\beta\Delta \sum_{n=1}^{\infty} (-1)^{n+1} n I_1(n\beta\Delta) K_0(n\beta\epsilon_0) & \text{for } \Delta < \epsilon_0, \end{cases} \quad (13a)$$

$$f_1 = \begin{cases} 1 - 2\beta\Delta \sum_{n=1}^{\infty} (-1)^{n+1} n K_1(n\beta\Delta) I_0(n\beta\epsilon_0) & \text{for } \Delta > \epsilon_0, \\ 2\beta\Delta \sum_{n=1}^{\infty} (-1)^{n+1} n I_1(n\beta\Delta) K_0(n\beta\epsilon_0) & \text{for } \Delta < \epsilon_0, \end{cases} \quad (13b)$$

and

$$f_0 = \begin{cases} 1 - 2 \sum_{n=1}^{\infty} (-1)^{n+1} \bar{K}(n\beta\Delta) I_0(n\beta\epsilon_0) & \text{for } \Delta > \epsilon_0, \\ \frac{\pi\Delta}{4T} \langle \text{sech}^2(\frac{1}{2}\beta\eta) \rangle - 2 \sum_{n=1}^{\infty} (-1)^{n+1} \bar{I}(n\beta\Delta) K_0(n\beta\epsilon_0) & \text{for } \Delta < \epsilon_0, \end{cases} \quad (14a)$$

$$f_0 = \begin{cases} 1 - 2 \sum_{n=1}^{\infty} (-1)^{n+1} \bar{K}(n\beta\Delta) I_0(n\beta\epsilon_0) & \text{for } \Delta > \epsilon_0, \\ \frac{\pi\Delta}{4T} \langle \text{sech}^2(\frac{1}{2}\beta\eta) \rangle - 2 \sum_{n=1}^{\infty} (-1)^{n+1} \bar{I}(n\beta\Delta) K_0(n\beta\epsilon_0) & \text{for } \Delta < \epsilon_0, \end{cases} \quad (14b)$$

where f_1 and f_0 are the static and the dynamic limit¹⁸ and

$$\bar{K}(z) = \int_0^{\infty} dx \text{sech}^2 x e^{-z \cosh x} \quad \text{and} \quad \bar{I}(z) = \int_0^z dy (z-y) I_0(y). \quad (15)$$

III. ELECTRON DENSITY OF STATES AND TUNNELING CURRENT

Making use of the Green's function given in Eq. (4), the electron density of states is given by⁷

$$N(E)/N_0 = \left\langle \text{Re} \frac{|E - \eta|}{[(E - \eta)^2 - \Delta^2]^{1/2}} \right\rangle$$

$$= \begin{cases} \frac{1}{\pi} \delta^{-1/2} \left\{ (x + \delta + 1) \Pi \left[-\frac{x - \delta + 1}{2\delta}, r \right] - \delta K(r) \right\} & \text{for } \delta - 1 < x < \delta + 1, \\ \frac{2}{\pi} [x^2 - (\delta - 1)^2]^{-1/2} \left\{ (x + \delta + 1) \Pi \left[-\frac{2}{x + \delta - 1}, r^{-1} \right] - \delta K(r^{-1}) \right\} & \text{for } x > \delta + 1, \end{cases} \quad (16a)$$

$$(16b)$$

when $\delta = \Delta/\varepsilon_0 > 1$, while for $\delta < 1$,

$$N(E)/N_0 = \frac{4}{\pi} [(1 + \delta)^2 - x^2]^{-1/2} \left[xK(r_1) + \Pi \left[-\frac{x - \delta + 1}{1 - x + \delta}, r_1 \right] + \Pi \left[\frac{x + \delta - 1}{x + \delta + 1}, r_1 \right] \right] \quad \text{for } 0 < x < 1 - \delta, \quad (17)$$

and for $x > 1 - \delta$ it is same as in Eqs. (16a) and (16b), where $x = |E|/\varepsilon_0$, $r = \frac{1}{2}[x^2 - (\delta - 1)^2/\delta]^{1/2}$ and

$$r_1 = [(1 - \delta)^2 - x^2/(1 + \delta)^2 - x^2]^{1/2}, \quad (18)$$

and $K(z)$, $\Pi(n, z)$ are the complete elliptic integral of the first kind and the third kind. The electron density of states is evaluated for $\varepsilon_0 = 0.16\Delta$, 0.92Δ , 1.08Δ , and 1.84Δ is shown as function of $x = E/\Delta$ in Fig. 5(a) and 5(b). When $\varepsilon_0 < \Delta$, the energy gap is given by $\Delta - \varepsilon_0$, while the maximum in the density of states is at $\Delta + \varepsilon_0$. We identify the apparent gap determined from the electric resistivity with $\Delta_a = \Delta + \varepsilon_0$, since the resistivity for not too low temperatures (i.e., $T > 0.5T_c$) is controlled by Δ_a .

When two SDW's are in contact, there will be a coupling between two SDW's in analogy to the Josephson coupling between two superconductors. This coupling energy is proportional to

$$F(T, \varepsilon_0/\Delta) = \pi T \Delta^2 \sum_{n=0}^{\infty} \left\langle [(\omega_n + i\eta)^2 + \Delta^2]^{-1/2} \right\rangle^2$$

$$= \Delta^2 \int_{\Delta - \varepsilon_0}^{\Delta + \varepsilon_0} dz \tanh \left[\frac{\beta}{2} z \right] R(z) I(z), \quad (19)$$

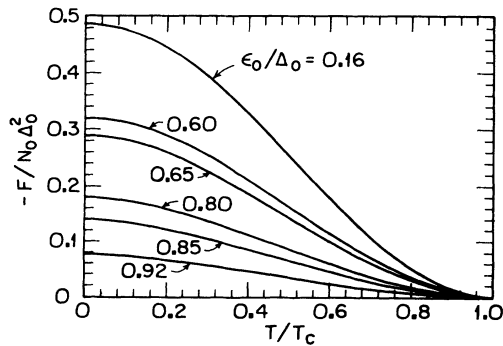


FIG. 2. Free-energy F normalized by $N_0(\Delta_0)^2$ is shown as function of T/T_c for a few ε_0/Δ_0 's.

where the lower limit of integration is $\Delta - \varepsilon_0$ when $\Delta > \varepsilon_0$ and 0 when $\Delta < \varepsilon_0$ and

$$R(z) = \text{Re} \left\langle [(z - \eta)^2 - \Delta^2]^{-1/2} \right\rangle$$

$$= \begin{cases} \frac{1}{\pi} (\Delta \varepsilon_0)^{-1/2} K(r) & \text{for } z > |\varepsilon_0 - \Delta|, \\ \frac{4}{\pi} [(\Delta + \varepsilon_0)^2 - z^2]^{-1/2} K(r_1) & \text{for } z < |\varepsilon_0 - \Delta|, \end{cases} \quad (20)$$

and

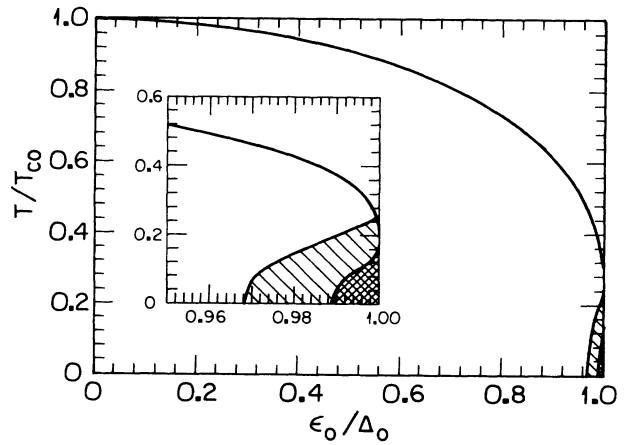


FIG. 3. Phase diagram for SDW and superconducting state is shown with the horizontal axis ε_0/Δ_0 . The shaded area is the superconducting area, two boundaries are for $T_{sc}/T_{c0} = 0.25$ and 0.15 , respectively, where T_{sc} is the superconducting transition temperature. In the insert, the region near $\varepsilon_0/\Delta_0 = 1$ is enlarged. As already noted by Yamaji, the superconducting state invades inside the original SDW region when two states meet.

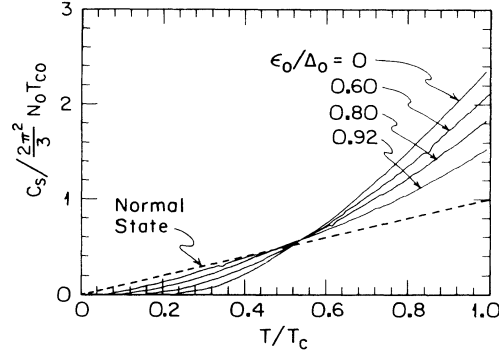


FIG. 4. Specific heat $C_s(\epsilon_0, T)$ is shown as function of T/T_c for a few ϵ_0/Δ_0 's.

$$I(z) = \text{Im} \left\langle \left[(z - \eta)^2 - \Delta^2 \right]^{-1/2} \right\rangle$$

$$= \begin{cases} \frac{1}{\pi} (\Delta \epsilon_0)^{-1/2} K(q) & \text{for } z > |\epsilon_0 - \Delta|, \\ \frac{2}{\pi} (\text{sgnz}) [(\Delta + \epsilon_0)^2 - z^2]^{-1/2} K(q^{-1}) & \text{for } z < |\epsilon_0 - \Delta|, \end{cases} \quad (21)$$

where r and r_1 have been already defined in Eq. (18) (now x has to be replaced by $x = z/\epsilon_0$), while

$$q = \frac{1}{2} \left[\frac{(1 + \delta)^2 - (z/\epsilon_0)^2}{\delta} \right]^{1/2}. \quad (22)$$

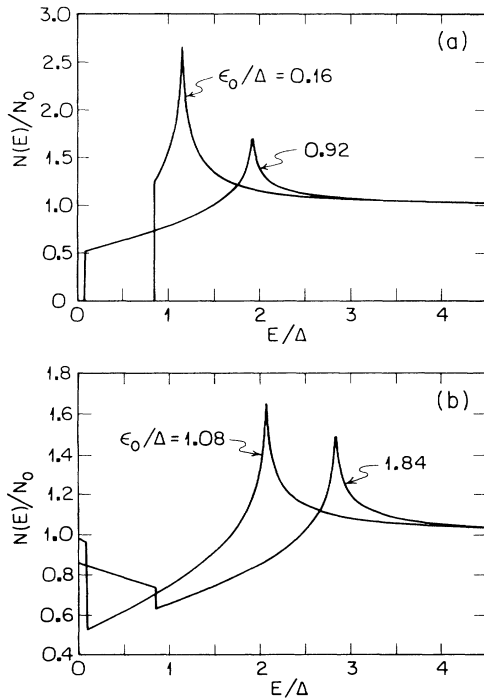


FIG. 5. (a) Electron density of states is shown as function of E/Δ when $\Delta > \epsilon_0$; $\epsilon_0 = 0.29\Delta$ and $\epsilon_0 = 0.16\Delta$. (b) Same for $\Delta < \epsilon_0$; $\epsilon_0 = 1.08\Delta$ and $\epsilon_0 = 1.84\Delta$.

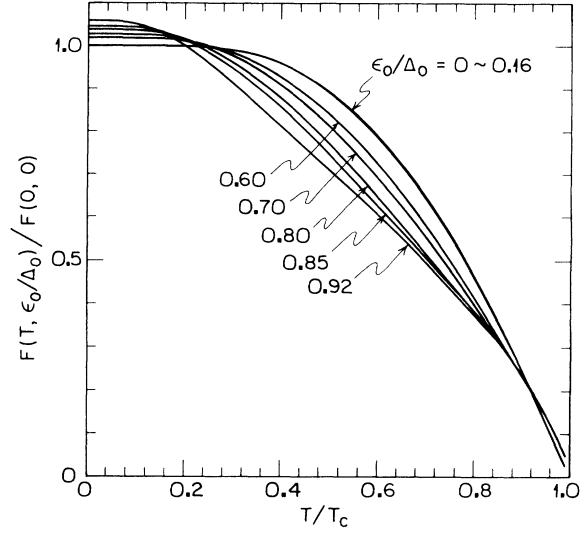


FIG. 6. The energy $F(T, \epsilon_0/\Delta)$ normalized by $F(0, 0) = \pi/4\Delta_0$ is shown as function of T/T_c for several ϵ_0/Δ_0 's.

In the limit $\epsilon_0 = 0$, $F(T, \epsilon_0/\Delta)$ reduces to

$$F(T, 0) = \frac{\pi}{4} \Delta \tanh \left[\frac{\Delta}{2T} \right]. \quad (23)$$

The F function normalized to the one at $T = \epsilon_0 = 0$ [$F(0, 0) = (\pi/4)\Delta_0$] is evaluated numerically for a few values of ϵ_0/Δ and shown in Fig. 6. In Fig. 7, we show $F(0, \epsilon_0/\Delta_0)/F(0, 0)$, which increases monotonically with increasing ϵ_0/Δ_0 . We note that the same integral appears in the pinning potential when $\epsilon_0 \neq 0$.

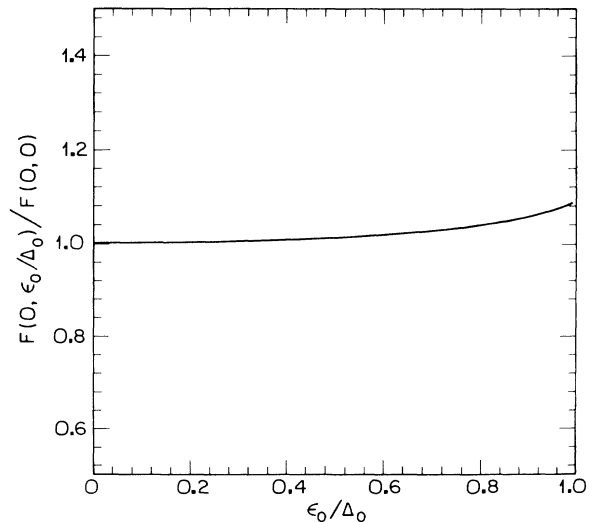


FIG. 7. $F(0, \epsilon_0/\Delta_0)/F(0, 0)$ is shown as function of ϵ_0/Δ_0 .

IV. DEPINNING ELECTRIC FIELD

Generalizing the model due to Fukuyama, Lee, and Rice²⁴ for SDW and for all temperatures we can calculate the threshold electric field corresponding to the depinning of SDW. It is important to distinguish the strong-pinning limit and the weak-pinning limit, though for pristine samples that contains little impurities the weak-pinning limit should apply due to weakness of the coupling between SDW and impurities.²⁵⁻²⁷ We do not write down the phason Hamiltonian here but summarize the result. In the strong-pinning limit the threshold electric field is given by²⁰

$$E_T^S(T_c)/E_T^S(0) = \frac{T_c^2}{\varepsilon_0 \Delta_0} \tanh \left[\frac{\varepsilon_0}{2T_c} \right] \left[F(0,0)/F(0,\varepsilon_0/\Delta_0) \right] \left[\sum_{n=1}^{\infty} (-1)^{n+1} n^2 K_0(n\beta\varepsilon_0) \right]^{-1}, \quad (26)$$

where we made use of the expressions

$$f_1|_{T \rightarrow T_c} \rightarrow (\beta\Delta)^2 \sum_{n=1}^{\infty} (-1)^{n+1} n^2 K_0(n\beta\varepsilon_0) \quad (27)$$

and

$$F(T,\varepsilon_0/\Delta_0) \rightarrow \frac{\pi\Delta^2}{4\varepsilon_0} \tanh \left[\frac{\varepsilon_0}{2T_c} \right], \quad (28)$$

where $\beta = T_c^{-1}$. Similarly, in the three-dimensional weak-pinning limit, the threshold field is given by¹⁸

$$E_T^W(0) = \frac{1}{6} (Q/en) \left[\frac{3}{2} (\pi N_0 V)^2 \right]^4 (\alpha \bar{v}^2 N_0)^{-3} \times (\eta^{-1} n_i)^2 [F(0,\varepsilon_0/\Delta_0)]^4 \quad (29)$$

and

$$E_T^W(T)/E_T^W(0) = [E_T^S(T)/E_T^S(0)]^4, \quad (30)$$

where $\alpha = \pi^2/3$, $\eta = v_2 v_3 / \bar{v}^2$ the anisotropy factor, and $\bar{v} = (1 + \bar{U})^{1/2} v$ is the phason velocity in the chain direction. The ratio $E_T^S(T)/E_T^S(0)$ is evaluated numerically for a few values of ε_0/Δ_0 and is shown as a function of T/T_c in Fig. 8. The temperature dependence of the

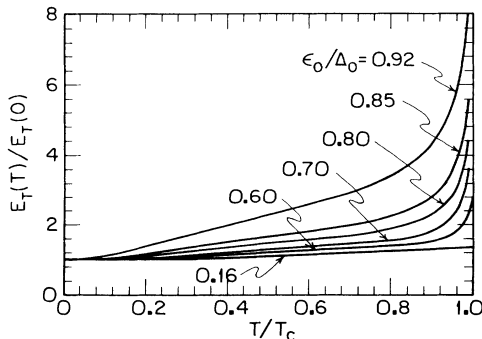


FIG. 8. $E_T^S(T)/E_T^S(0)$ is shown as function of T/T_c for a few ε_0/Δ_0 's.

$$E_T^S(0) = (Q/e)(n_i/n)(\pi N_0 V)^2 F(0,\varepsilon_0/\Delta_0) \quad (24)$$

and

$$E_T^S(T)/E_T^S(0) = [F(T,\varepsilon_0/\Delta)/F(0,\varepsilon_0/\Delta_0)] f_1^{-1}, \quad (25)$$

where both $F(T,\varepsilon_0/\Delta)$ and f_1 have been already defined in Eqs. (19) and (13), respectively. Here, $Q = 2p_F$, and n_i , n , and v are the impurity density, the electron density, and the impurity potential, respectively. At $T=0$ K, $E_T^S(0)$ increases with increasing ε_0 , since $E_T^S(0)$ is proportional to $F(0,\varepsilon_0/\Delta_0)$ (see Fig. 7). In particular at $T = T_c$, Eq. (25) simplifies

threshold field increases clearly as ε_0 increases. This stronger temperature dependence comes mostly from the stronger reduction¹⁸ of f_1 for $T > \frac{1}{2}T_c$, though both f_1 and $F(T,\varepsilon_0/\Delta)$ become more temperature dependent for small reduced temperatures as ε_0 increases. In particular, the experimental data²¹ of the threshold electric field in SDW of quenched $(\text{TMTSF})_2\text{ClO}_4$ appears to be described if we choose $\varepsilon_0/\Delta_0 \simeq 0.8$ and in the weak-pinning limit. The value $\varepsilon_0/\Delta_0 \simeq 0.80$ for quenched $(\text{TMTSF})_2\text{ClO}_4$ is consistent with $\varepsilon_0 = 17$ K deduced from Yamaji's model for relaxed $(\text{TMTSF})_2\text{ClO}_4$ in order to describe the field-induced SDW phase transition.^{12,14} Since relaxed $(\text{TMTSF})_2\text{ClO}_4$ does not undergo the SDW transition, this implies that $\Delta_0 \leq 17$ K or $T_{c0} = 9$ K (i.e., the hypothetical SDW transition temperature in the limit of perfect nesting $\varepsilon_0 = 0$) for $(\text{TMTSF})_2\text{ClO}_4$. Then the transition temperature T_c of quenched $(\text{TMTSF})_2\text{ClO}_4$ depends on the quenching rate.^{28,29} Therefore, it is, in principle, possible to study systematically the effect of imperfect nesting; a slower quenching means lower T_c and larger imperfect nesting ε_0/Δ_0 .

So far, we are considered only with the threshold electric field in SDW. In principle, a parallel analysis is possible in CDW. However, due to the extra temperature dependence of the threshold field most likely associated with thermal fluctuation,³⁰ a clear-cut comparison between theory and experiment is rather difficult in CDW. Therefore, SDW appears to provide a unique possibility to explore the effect of imperfect nesting through the temperature dependence of the threshold field. A similar test of theory may be carried out for $(\text{TMTSF})_2\text{PF}_6$ under pressure as well.

ACKNOWLEDGMENTS

We would like to thank K. Nomura for sending us a copy of Ref. 21 prior to publication and for useful correspondence, which gave an early impetus to this work. This work is supported by the National Science Foundation under Grant No. DMR 89-15285.

- *Present address: T-11, MS-B 262 Los Alamos National Laboratory, Los Alamos, NM 87545.
- ¹P. Monceau, in *Electronic Properties of Inorganic Quasi-One-Dimensional Materials*, edited by P. Monceau (Reidel, Dordrecht, 1985), p. 139.
- ²J. Richard, H. Salva, M. C. Saint-Lager, and P. Monceau, *J. Phys. (Paris) Colloq.* **44**, C3-1685 (1983); M. C. Saint-Lager, Thesis (3eme cycle), Université de Grenoble, 1983 (unpublished).
- ³P. M. Horn and Guiddoti, *Phys. Rev. B* **16**, 491 (1977).
- ⁴K. Maki, *Phys. Rev. B* **41**, 9308 (1990).
- ⁵B. Horovitz, M. Weger, and H. Gutfreund, *Phys. Rev. B* **9**, 1246 (1974); B. Horovitz, H. Gutfreund, and M. Weger, *ibid.* **12**, 3174 (1975).
- ⁶K. Yamaji, *J. Phys. Soc. Jpn.* **51**, 2787 (1982); **52**, 1361 (1983).
- ⁷X. Huang and K. Maki, *Phys. Rev. B* **40**, 2575 (1989).
- ⁸A. Briggs, P. Monceau, M. Nuñez-Regueiro, J. Peyrard, M. Ribault, and J. Richard, *J. Phys. C* **13**, 2117 (1980).
- ⁹T. Ekino and J. Akimitsu, *Jpn. J. Appl. Phys. Suppl.* **26**, 625 (1987).
- ¹⁰S. Tomić, J. R. Cooper, W. Kang, D. Jérôme, and K. Maki, *J. Phys. I (France)* **1**, 1603 (1991).
- ¹¹D. Jérôme, A. Mazaud, M. Ribault, and K. Bechgaard, *J. Phys. (Paris) Lett.* **41**, L195 (1980).
- ¹²K. Yamaji, *J. Phys. Soc. Jpn.* **54**, 1034 (1985); *Synth. Met.* **13**, 29 (1986).
- ¹³D. Poilblanc, G. Montambaux, M. Héritier, and P. Lederer, *J. Phys. C* **19**, L321 (1986).
- ¹⁴A. Virosztek, L. Chen, and K. Maki, *Phys. Rev. B* **34**, 3371 (1986).
- ¹⁵Y. Hasegawa and H. Fukuyama, *J. Phys. Soc. Jpn.* **55**, 3978 (1986).
- ¹⁶G. Montambaux, *Phys. Rev. B* **38**, 4788 (1988).
- ¹⁷K. Maki and A. Virosztek, *Phys. Rev. B* **41**, 557 (1990).
- ¹⁸X. Huang and K. Maki, *Phys. Rev. B* **42**, 6498 (1990).
- ¹⁹W. Kang, S. Tomić, J. R. Cooper, and D. Jérôme, *Phys. Rev. B* **41**, 4862 (1990); W. Kang, S. Tomić, and D. Jérôme, *ibid.* **43**, 1264 (1991).
- ²⁰K. Maki and A. Virosztek, *Phys. Rev. B* **42**, 655 (1990).
- ²¹T. Shimizu, K. Nomura, T. Sambongi, H. Anzai, N. Kinoshita, and M. Tokumoto, *Solid State Commun.* **78**, 697 (1991); T. Sambongi *et al.*, *ibid.* **72**, 817 (1989).
- ²²S. Tomić, J. R. Cooper, D. Jérôme, and K. Bechgaard, *Phys. Rev. Lett.* **62**, 2466 (1989).
- ²³See, for example, A. A. Abrikosov, L. P. Gor'kov, and I. E. Dzyaloshinskii, *Method of Quantum Field Theory in Statistical Physics* (Dover, New York, 1975), pp. 303–306.
- ²⁴H. Fukuyama and P. A. Lee, *Phys. Rev. B* **17**, 535 (1978); P. A. Lee and T. M. Rice, *ibid.* **19**, 3970 (1979).
- ²⁵P. F. Tua and J. Ruvalds, *Phys. Rev. B* **32**, 4660 (1985).
- ²⁶A. Virosztek and K. Maki, *Phys. Rev. B* **37**, 2028 (1988).
- ²⁷I. Tüttö and Zawadowski, *Phys. Rev. Lett.* **60**, 1442 (1988).
- ²⁸S. Tomić, D. Jérôme, P. Monod, and K. Bechgaard, *J. Phys. (Paris) Colloq. C* **44**, 3-1083 (1983).
- ²⁹K. Nomura (private communication).
- ³⁰K. Maki, *Phys. Rev. B* **33**, 2852 (1986).